Optical remote sensing of submerged aquatic vegetation: opportunities for shallow clear water streams

Fleur Visser*, Caroline Wallis, Anne Sinnott
Institute of Science and the Environment, University of Worcester,
Henwick Grove, Worcester, WR2 6AJ, United Kingdom

*Corresponding author. Tel.: +44 1905 855236. E-mail address: f.visser@worc.ac.uk.

Running title: Remote sensing of submerged vegetation in clear streams

Keywords: Submerged aquatic vegetation, shallow rivers, optical remote sensing, object-based image analysis, very high resolution image data

Abstract

Remote sensing has rarely been used as a tool to map and monitor submerged aquatic vegetation (SAV) in rivers, due to a combination of insufficient spatial resolution of available image data and strong attenuation of light in water through absorption and scattering. The latter process reduces the possibility to use spectral reflectance information to accurately classify submerged species. However, increasing availability of Very High Resolution (VHR) image data may enable the use of shape and texture features to help discriminate between species by taking an Object Based Image Analysis (OBIA) approach, and overcome some of the present limitations.

This study aimed to investigate the possibility of using optical remote sensing for the detection and mapping of SAV. It firstly looked at the possibilities to discriminate submerged macrophyte species based on spectral information only. Reflectance spectra of three macophyte species were measured *in-situ* across a range of submergence depths. The results showed that water depth will be a limiting factor for the classification of species from remote sensing images. Only Spiked Water Milfoil (*Myriophyllum spicatum*) was indicated as spectrally distinct through ANOVA analysis, but subsequent Jeffries-Matusita distance analysis did not confirm this. In particular Water Crowfoot (*Ranunculus fluitans*) and Pondweed (*Potamogeton pectinatus*) could not be discriminated at 95% significance level. Spectral separability of these two species was also not possible without the effect of an overlying water column.

Secondly, the possibility to improve species discrimination, using spatial and textural information was investigated for the same SAV species. VHR image data was acquired with a Near Infrared (NIR) sensitive DSLR camera from four different heights including a telescopic pole and a Helikite UAS. The results show that shape and texture information can improve the detection of the spectrally similar Pondweed and Water Crowfoot from VHR image data. The best performing feature 'length/width ratio of sub-objects' was obtained through expert knowledge. All of the shape and texture based features performed better at species differentiation than the spectrally based features.

In conclusion this study has shown that there is considerable potential for the combination of VHR data and OBIA to map SAV in shallow stream environments, which can benefit species monitoring and management.

Introduction

Collecting data on submerged aquatic vegetation (SAV) from fluvial environments, which sufficiently represent spatial variation along a river reach, is difficult to achieve and often requires destructive and labour-intensive fieldwork (e.g. Flynn et al., 2002). Methods to obtain information remotely could therefore be of great benefit to the field of river science, including ecohydraulics. However, a combination of insufficient spatial resolution of image data and strong attenuation of light in water through absorption and scattering has long been a barrier for the application of remote sensing technology to study fluvial environments (Gilvear et al., 2007; Marcus and Fonstad, 2008). This paper describes a project that applies a set of novel remote sensing techniques to map SAV, which could help overcome some of these limitations.

Remote sensing has so far rarely been used as a tool to map and monitor submerged aquatic vegetation in rivers (Marcus and Fonstad, 2008). A recent study by Lee et al. (2011) is one of the first to look at the feasibility of using airborne hyperspectral image data to map SAV communities in rivers. They studied the separability of four vegetation types in small rivers in western Nevada, US, which included submerged brown and green filamentous algae communities. In the UK Hill et al. (2009) were some of the first to attempt estimating submerged vegetation biomass (Water Crowfoot) from image data taken with an airborne hyperspectral sensor. They did this for the River Frome chalk stream. Although a reasonable estimate could be made, the success of this analysis was severely limited by the quality and spatial resolution of the data (>1m) (Visser and Hill, 2011). Clearly further work is required in this field.

While for terrestrial applications light in the near infrared wavelengths (NIR) is particularly useful for the detection of variation in vegetation cover, the absorption characteristics of water limit its use for SAV. As a result of both absorption by water and scattering by particles, light is attenuated with distance travelled through the water column. In the optical range of the electromagnetic spectrum NIR is more strongly absorbed by water than the visible wavelengths (VIS). NIR can therefore only be used in image data of very shallow aquatic environments (< ~1m) to provide any information about bottom features. It also means that in sufficiently shallow aquatic environments variation in recorded NIR reflectance does not only reflect variation in vegetation types or condition, but also variation in the depth of the plant below the water surface. When applying optical imagery to map SAV, this results in an unfortunate situation, which is described by Hedley et al. (2012) as 'environmentally limited remote sensing'. Variation in depth, variation in the reflectance signatures of the bottom substrate or cover types and potentially other factors such as water clarity, together contribute to overall variation in the signal recorded by an image sensor and can lead to an overlap between two or more mapped vegetation classes.

Hedley et al. (2012) focussed on such environmental limitations in Australian marine environments. Generally more work has been done on remote sensing of SAV in marine environments and various attempts have been made to resolve complications of submerged situations. O'Neill et al. (2011) for example used information about submergence depth to adjust above water reflectance spectra for attenuation influence, using the empirical water attenuation correction by Maritorena et al. (1994). O'Neill et al. (2011) had access to a depth dataset and managed to produce a 97% overall classification accuracy for Eelgrass detection. Depth data of sufficient quality is however not usually available and certainly not of the detail required for fluvial environments. Lidar and radar data which work for terrestrial situations again do not (yet) perform well enough in submerged fluvial conditions (e.g. Wang and Philpot, 2007). Important progress is being made with the application of inversion of modeling of bio-optical models (e.g. Dekker et al. (2011) for marine environment and Giardino et al. (2012) for lacustrine settings). Legleiter and Roberts (2009) explored the potential of inverse modelling with regards to accuracy and precision methods for fluvial environments, using data simulated with a forward image model (FIM). They found they methods would be suitable for depth retrieval. However, data and analysis techniques are still insufficient to successfully apply them in fluvial environments.

The foregoing overview identified how a combination of insufficient spatial and spectral resolution of available image data, has so far ruled out their use for studies of smaller rivers (width < 10m). However ongoing improvements of image data collection and image analysis techniques are finally changing this situation. Unmanned Aerial Systems (UAS), which are small, low-altitude remote sensing platforms such as small fixed winged planes or mini-helicopters, are rapidly developing into relatively cheap and logistically flexible means to obtain Very High Resolution (VHR) multi-spectral image data. When classifying a remote sensing image to obtain maps of submerged environments (e.g. SAV or river bed morphology) VHR data has the advantage that it can generate detailed information on aspects of shape, structure and texture of the target surface. Using so-called ‘Object Based Image Analysis’ (OBIA) techniques this information can be incorporated in the image analysis process to improve an image classification originally based on spectral information only (e.g. Van der Werff and Van der Meer, 2008 and Laliberté and Rango, 2009). While conventional image analysis techniques derive information about the target spectral reflectance on a pixel by pixel basis, OBIA first segments the image data into spectrally homogenous objects. For each object it then quantifies feature values such as shape (e.g. roundness or length/width ratio), internal texture and characteristics of adjacent objects (e.g. contrast to neighbouring object). When such additional object feature values are included in the analysis algorithm they can considerably improve image classification (e.g. Blaschke et al., 2011).

The study aimed to establish application of remote sensing methods for fluvial environments and better appreciate the inherent limitations as identified by Hedley et al. (2012). This was done by meeting the following two objectives:

- Determine the possibility to discriminate between three submerged macrophyte species based on spectral information only.
- Determine whether discrimination of the same species could be improved using spatial and textural information obtained from VHR image data.

Methods

Introduction

Statistically discriminating between surface (cover) types based on spectral information, lies at the basis of classification of remote sensing image data. For this purpose spectral information about the cover types is usually obtained from a training sample of pixels in the image. If separability between the samples is higher, cover types can be mapped from the image more reliably. In order to check whether classification is possible in the first place and to find the optimal wavelength bands (or band combinations) to do this, a considerable number of studies have also investigated separability of sets of individual spectra from cover types measured *in-situ* (e.g. Vahtmäe et al., 2006; Karpouzli et al., 2004; O'Neill et al., 2011; Lee et al., 2011). In this study a GER1500 hand-held field spectroradiometer was used to collect reflectance spectra *in-situ* from the three submerged macrophyte species across a range of submergence depths.

Remote sensing image classification processing time increases with the number of spectral bands associated with a pixel, so techniques to assess separability between classes usually involve a reduction in data dimensionality. A range of techniques have been applied to determine separability of cover types, based on samples of in situ reflectance spectra (e.g. Lee et al., 2011; O’Neill et al., 2011; Adam and Mutanga, 2009). This suggests that there is no consensus on what method is most suitable. This observation is confirmed by Adam and Mutanga (2009) and Yang et al. (2005). Here we use the methodology of Adam and Mutanga (2009), who took a hierarchical approach to reduce the dimensionality of their data before determining species separability. One-way ANOVA was used with a post-hoc Scheffé test to determine for each wavelength band which macrophyte pairs were significantly different. This was followed by Classification And Regression Trees (CART) analysis (Breiman et al., 1984) to select the most suitable bands for species discrimination.

A trained observer will be able to distinguish between Pondweed and Water Crowfoot by looking at their photographs despite their similar green colour. Their interpretation or ‘classification’ of the image will therefore involve more than the clustering of spectral values, as done in the first part of this study. OBIA attempts to simulate these additional human cognitive processes in order to improve image classification based on clustering of spectral values only. Recent studies by Phinn et al. (2012) and Urbanski et al. (2009) have shown the benefit of this kind of approach for marine environments.The second part of this study therefore investigates the possibility to improve discrimination of the same three SAV species from image data, using spatial and textural information in addition to the spectral information. VHR image data for this part of the study is acquired with a

Near Infrared (NIR) sensitive DSLR camera. Images are taken from four different heights, in order to understand how the OBIA approach is affected by the scale of the image data. The platforms used to achieve this include a telescopic pole and a Helikite UAS.

Study sites

The field sites for this study were located along two UK chalk streams: the River Wylye in Wiltshire and the River Frome in Dorset. These calcareous groundwater-fed streams were selected because of their exceptional water clarity and abundance of a range of macrophyte species. Most data were obtained from the River Wylye at Steeple Langford where it flows through the Langford Trust nature reserve in Wiltshire. Additional data was collected from a distributary of the River Frome near Wool in Dorset. The sites were physically very similar, with a stream width of around 5m and a maximum water depth at time of sampling of around 50cm. Although this study involves one particular type of stream only, the techniques and issues discussed are likely to apply to a much wider range of clear water streams with SAV and to some extent also shallow lake environments.

The study focuses on three macrophyte species commonly found in the chalk streams: Water Crowfoot (*Ranunculus fluitans*), Pondweed (*Potamogeton pectinatus*) and Spiked Water Milfoil (*Myriophyllum spicantum*). Water Crowfoot is a keystone species of high conservation value for chalk stream environments. The habitats they form are protected under the European Union Habitats and Species Directive (92/43/EEC) (O'Hare et al., 2010). Management of the species is therefore a trade-off between conservation and growth control for fisheries and flood management. Remote sensing could make an important contribution to improved management practices. The other two species were chosen because of their relative abundance at the field sites and because pondweed is spectrally very similar to Water Crowfoot, but structurally rather different, while the opposite is the case for Water Milfoil.

Spectral measurements of submerged aquatic vegetation

To collect reflectance spectra from three submerged macrophyte species, measurements took place with a GER1500 hand-held field spectroradiometer over several days in late August and early September of 2009 and 2010 at both field sites. Due to limited access to the river and limited availability of specific vegetation species at different depths purposive sampling was applied to obtain submerged vegetation spectra at a range of submergence depths. To obtain spectra of vegetation without water column influences multiple layers of vegetation were piled on black painted canvas. The GER1500 was held at nadir 50cm above the water surface or canvas. The instrument has a 3° field of view so the area measured on the target has a 2.6 – 4.0cm diameter (depending on submergence depth), which is assumed sufficient to obtain representative spectral information from the dense vegetation stands. Sampling was carried out on cloud-free days within 2 hours of solar noon. Spectral averaging of 10–30 spectra per sample was performed to ensure optimal signal-to-noise ratio. A white reference Spectralon calibration panel of 99% reflectance was used every 5 to 10 samples to offset any change in the atmospheric condition and irradiance of the sun. Reflectance was calculated by dividing macrophyte radiance by radiance from the Spectralon surface.

ANOVA and CART Analysis species discrimination

To analysis species discrimination we used the methodology of Adam and Mutanga (2009). They took a hierarchical approach to reduce the dimensionality of their data before determining species separability. This first involves a statistical test of differences in mean reflectance values for all combinations of two macrophyte species at each measured wavelength (350 to 1050 nm):

$$H0 : \mu1(i) = \mu2(i) = \mu3(i)$$
$$H1 : \text{at least one } \mu(i) \text{ is different}$$

where μ1-3 represent the mean reflectance of the 3 macrophyte species and i denotes the spectral wavelength band. One-way ANOVA was used with a post-hoc Scheffé test to determine for each wavelength band which macrophyte pairs were significantly different. ANOVA was tested for 99% and 95% confidence levels ($p < 0.01$ and $p < 0.05$). For each wavelength band the number of significantly different macrophyte species combinations were counted (in this case max. 3) to determine the wavelength bands most suitable for spectral discrimination. The one-way ANOVA coupled with a post-hoc pair-wise comparison resulted in a frequency plot of statistically significant mean reflectance values for each wavelength.

Although significant difference for the ANOVA test indicates at which wavelengths species are most likely to be spectrally different, it does not guarantee separability of the macrophyte species based on individual wavelength bands from this region. A measure for correct classification of the vegetation types from image data using a single or combination of multiple bands can be determined by calculating Jeffries–Matusita (J–M) distance values. However, it is very time consuming to calculate the distance measure for all possible combinations of the bands identified by ANOVA. Adam and Mutanga (2009) therefore performed a further step to select the most suitable bands for species discrimination, using the Classification And Regression Trees (CART) approach (Breiman et al., 1984). CART is a form of binary recursive partitioning that permits accurate prediction or classification of cases, using both continuous and categorical variables. Training data is used to identify 'splitting' variables based on an exhaustive search of possible variable combinations. Repeated partitioning of the data with additional variables occurs until criteria for predictive accuracy are met. This automatically results in the optimal number of bands for separation of all classes/species.

For this study we did CART analysis using the bands from 99% confidence level regions as input and compared the results with CART analysis using the full set of bands to confirm the benefit of initial band selection through ANOVA. Each tree/model was validated with a test sample of at least 25%. Because we were particularly interested in the possibility to separate the spectrally very similar Pondweed and Water Crowfoot, additional CART band selection was performed including these two species only and the results will also be presented.

Finally Jeffries–Matusita (J–M) distance values were calculated for the wavelength band combinations selected by the CART method. To determine to what extent improvement of species separation was achieved at the different stages of the analysis process, we also calculated J-M values for 5 sets of 5 band combinations ranging from 2-6 bands which were randomly selected from the ANOVA 99% confidence level regions only, as well as J-M values for 5 sets of 5 band combinations ranging from 2-6 bands selected at random from the 741bands included in the analysis. The square of the J–M distance values ranges between 0 and 2, with larger J–M distance values indicating greater separability between group pairs. Values greater than 1.9 indicate that the sample pairs have good separability (ENVI, 2004).

$$J - M_{ij} = \sqrt{2(1 - e^{-\alpha})} \qquad 1$$

With

$$\alpha = \frac{1}{8}\left(\mu_i - \mu_j\right)^T \left(\frac{C_i + C_j}{2}\right)^{-1} \left(\mu_i - \mu_j\right) + 2\ln\left(\frac{\left(\frac{1}{2}\right)\left|C_i + C_j\right|}{\sqrt{\left|C_i\right| x \left|C_j\right|}}\right) \qquad 2$$

Where i and j are the two species compared; C_i= covariance matrix of the spectral response of i; μ_i = the mean vector of signature of i; T = transposition function; $\left|C_i\right|$ = the determinant of C_i.

Collection of VHR image data

Next we tested the usefulness of a range of image object features such as shape and texture to distinguish between macrophyte species in shallow rivers. We focused only on the two spectrally most similar macrophyte species Water Crowfoot and Pondweed. The analysis was applied to a set of four multi-spectral images, which included stands of both species. All images were taken with the same camera from four 'platforms' at different heights above the water surface in order to evaluate the applicability of shape and texture features for species detection across a range of scales. The platforms included a tripod located in the river near a bridge at 1.5m elevation (location: 'from tripod'), from a bridge at 3m (location: 'from bridge',) from a telescopic pole at 5.4m (location: 'from pole',) and from a Helikite UAS (a combined helium balloon and kite) at about 5m elevation (location: 'from helikite',).

Despite strong absorption of NIR light in water, spectral signatures of submerged macrophytes measured with the GER1500 field spectroradiometer, indicated that light in these wavelengths may be useful in image classification (Visser and Wallis, 2010). Initial inspection of NIR images also showed that plant structure and shape features appeared more strongly pronounced in this wavelength region. Because sufficiently light-weight multispectral sensors suitable for small UAS-s are not available yet, multi-spectral images have been created with a Fujifilm IS-Pro NIR sensitive DSLR camera on a layer by layer basis, taking repeated photos of the same location and stacking these subsequently using GIS software. A NIR blocking filter was used on the camera to obtain Red, Green and Blue image bands, A VIS blocking filter was used to obtain a band covering most of the NIR spectrum (R72) and a bandpass filter was used to obtain a narrow NIR wavelength band round 710nm (NIR (BP1)). Figure 1 shows the filter transmission spectra and their specifications are as follows:

- R, G, B: MaxMax X-Nite CC1 NIR blocking filter (centre: 483nm; 50% transmission: 325nm, 645nm)
- NIR(R72): Hoya R72 VIS blocking filter (<720nm)
- NIR(BP1): MaxMax XNiteBPB band pass filter (650nm to 787nm; 5% low cut – 5% high cut)

5-Band image composites were created by overlaying and rectifying the different wavelength bands based on manually located ground control points in each image. Parts of the scenes not covered by all image bands were cropped before further analysis. No suitable photos were collected with the NIR(BP1) filter from the Helikite platform, so this band is missing from the 'from helikite' image stack.

Image segmentation and object analysis

To obtain image objects and enable calculation of meaningful feature values from these, all images were segmented in Trimble eCognition image analysis software (Trimble, 2010) at two levels. A first segmentation level was created using the Red and NIR(R72) bands only, which was suitable for delineation of vegetated areas. At a scale parameter of 200 groups of objects best followed the outlines of the main vegetation patches, while individual objects fully delineated the majority of smaller patches (± 25cm diameter). 'Shape' and 'compactness' parameters were chosen as 0.5 and 0.1, since at this level object delineation should be determined by both shape and spectral characteristics of the data, while the shape of the objects should be able to take on any form (i.e. low compactness). Next the image objects at this first level were sub-segmented at a second level to obtain objects that delineated the more detailed structure of the plants. The same image bands were used at this level, but a scale parameter of 20 and shape and compactness parameters of 0.9 and 0 were chosen. The latter two parameters indicate that object delineation was mostly determined by its shape and could take on any form. For all images these segmentation settings resulted in the creation of rather elongated sub-objects, clearly representing the 'hair-like' shape of some of the macrophytes (see image close up in Figure 2).

A large number of features are available in eCognition to describe the shape and texture of image objects and many more can be 'designed' by the user. Due to their large number, selection of the most suitable features to classify species can involve similar procedures as used for spectral band selection. However the user can also use expert opinion to select the most meaningful features based on visual interpretation of the image data. A combined approach was applied for this study. The following two features were developed based on expert opinion and thought to describe the structural difference between macrophyte species:

1) Mean length/width ratio of sub-objects.

This feature value is obtained by calculating the length/width ratio for all level two objects and averaging these within each first level object. The value seems to quantify the presence of a 'hair-like' structure in particularly Water Crowfoot patches.

2) Mean standard deviation red of sub-objects.

This feature value is obtained by calculating the standard deviation of pixel values for all level two objects and averaging these within each first level object. The value seems to represent a relatively strong spectral difference between the stems and leaves of the Water Crowfoot plants.

A further selection of features for this analysis was taken from a range of texture measures that are standard included in the eCognition software. The eCognition 'Feature Selection Tool' used for this purpose determines the most suitable features from a given selection. This resulted in a selection of three Grey Level Co-occurrence Matrix features (GLCM), which are texture measures as described by Haralick et al. (1973). The measures quantify the amount of variability between adjacent pixels that make up an object. In this case the measures for contrast, dissimilarity and homogeneity were tested. The various types of texture features and their different calculation methods tend to produce strongly correlated values and are likely to result in similar difference estimates.

For the objects representing each of the species the following range of feature values were calculated and exported into SPSS for further difference analysis:

- Mean Length/ Width Sub-objects
- Mean standard deviation red of sub-objects
- GLCM Contrast (quick 8/11 all dir.)
- GLCM dissimilarity (quick 8/11 all dir.)
- GLCM homogeneity (quick 8/11 all dir.)

In addition to this the average reflectance values for the objects in each band were calculated, exported and compared in the same manner. Because the number of Pondweed objects for some images were relatively small, a non-parametric Mann-Whitney U test was executed to determine to what extent there was a significant difference between object feature values of each macrophyte species.

Results

Spectral species discrimination

Table 1 shows a summary of the sample numbers and depth ranges measured for each of the macrophyte species. Each sample has a spectral range of 350 - 1050nm and a sampling interval of 1.5nm. An example spectrum is shown in Figure 3, which also shows the attenuation coefficient of water (K_d). Suspended load is mostly absent from the sampled streams, so no water quality adjustments were made.

The results of the ANOVA analysis for the submerged vegetation spectra and those of vegetation put onto the canvas are presented in Figures 4 and 5. The dark grey histograms indicate the wavelength ranges where significant differences were found between combinations of two or more different macrophyte species with a 99% confidence level. The light grey parts of the histograms indicate differences at 95% confidence level. The ANOVA test resulted in a slightly narrower range of suitable wavelengths for the submerged vegetation spectra compared to those estimated for vegetation taken out of the water. For submerged spectra differences at 95% significance level were only found for the 500 to 600nm and the 850 to 950nm wavelength regions (Figure 4). For 99% significance level this range was reduced to a region of visible green light between 525 and 576nm and a very narrow section of the IR between 913 and 926nm. The latter finding is quite remarkable as the IR wavelengths are expected to be strongly affected by water absorption. The range of significant spectra measured on the canvas is wider (Figure 5), but considerable areas with too much overlap between species remain. Similar to the submerged spectra significant differences are found in the VIS wavelengths between 500 and 600nm. However, the range of significant NIR bands is different. Significant wavelengths for spectra on canvas start at the beginning of the red edge (from 691nm) and become less pronounced from 823nm onwards. The secondary y-axis in both figures indicates the number of significant species combinations for each grey wavelength region. For both sets of spectra only significant differences were found between Milfoil and Pondweed or Milfoil and Crowfoot. Differences between Pondweed and Crowfoot were not significant at 95% for any of the wavelengths both above and below the water surface.

Table 2 shows the combined results of the CART and J-M analysis for the submerged vegetation spectra. The table lists the J-M distance values from band selection resulting from CART as well as the best performing combinations of 2 to 6 bands, which were randomly drawn from the significant ANOVA range and the full data set. Results of CART analysis performed on Pondweed and Crowfoot data only are also included. Best performing band combinations are highlighted. Table 3 shows the same information for the vegetation spectra measured on canvas. The J-M distance analysis results show that despite the significant difference between species for individual wavelengths in the ANOVA analysis, actual separability of the species is not necessarily possible. Complete separability of Water Milfoil and either of the other two species is possible when the spectra are measured without the influences of water. However, J-M values only get up to 1.44 for separability between Water Crowfoot and Pondweed. The J-M values become lower when the vegetation is covered by a variable water layer. Better results are achieved when the number of bands used in the analysis increases, however, attempts using up to 6 bands did still not result in the recommended minimum J-M distance of 1.9. For 6 bands highest values of 1.87 were obtained for Pondweed and Water Milfoil, both other combinations had lower values: 1.66 for Crowfoot and Milfoil and 1.62 for Pondweed and Crowfoot. The latter value was obtained for a combination with one band less.

OBIA species discrimination

Figures 6A-D show the outlines of the first segmentation level of objects in each image taken from the four different platforms. Objects representing Pondweed and Water Crowfoot were manually selected and are outlined in white and grey respectively. Table 4 shows the total number of objects for each of the two species available for analysis. Table 5 shows the significance levels of the Mann-Whitney U test for difference in object feature values between both macrophyte species, as observed from each platform. More detailed information about the distribution of each sample is shown in the boxplots of Figures 7A-F. The data indicates that the best results for separating the macrophytes were achieved with the highest resolution data. Objects from the image taken from a tripod just above the water surface show significant differences for all object shape and texture features tested. The lowest p values were obtained for the difference test using some of the spectral band values only (i.e. red, BP1 and R72+BP1). All lower resolution data show fewer significantly different object features. The feature that performs best is the ‘mean length/width ratio of the sub-objects’. The remaining texture features all perform similarly. Figures 7 A-H show boxplots that illustrate the distribution of values for a selection of 8 features (red, green, blue, BP1, R72, mean length/width ratio sub-objects, mean standard deviation sub-objects and GLCM contrast).

Discussion and implications

Spectral species discrimination

The results showed that water depth will be a limiting factor for the classification of species from remote sensing images. Spiked Water Milfoil was indicated as spectrally distinct from the other species across the observed range of water depths with ANOVA analysis, but this was not confirmed by Jeffries-Matusita distance analysis. In particular Water Crowfoot and Pondweed could not be discriminated at 95% significance level. J-M distance analysis values confirmed these observations. The latter two species are spectrally so similar that they could not be discriminated without the effect of an overlying water column either.

Both submerged macrophytes and those taken out of the water on the canvas show significant differences in the VIS wavelength range between 500 and 600nm. This range corresponds with useful bands found by O'Neill et al. (2011) who found that most marked differences between benthic classes occurred in the green spectral range between 500 and 600 nm, which coincides with lower K_d values. It also coincides with the photosynthetic pigment absorption minimum between that lies between 555 and 565. The position of the significant NIR range is rather different for each of the two data sets. The range including the red-edge, found for the spectra on canvas, corresponds with findings for most terrestrial vegetation species, which show most variation around this region. The same NIR region does not result in significant differences for the submerged spectra, which was expected considering the high variability in this wavelength region due to the increased K_d. Remarkably however, a small region of wavelengths between 850 and 950nm is selected in the ANOVA analysis and some of the NIR wavelengths contribute to the combinations that result in best separability. For emergent species Adam and Mutanga (2009) also identified several wavelengths in this part of the NIR as most useful for discrimination between vegetation species.

The results indicate that for accurate classification of any of the submerged macrophytes more than 6 wavelength bands will be required. Depth clearly has an influence here as for the spectra measured on canvas sufficient distance values were achieved for two out of the three species combinations with three bands or less. Comparisons with results from other studies are difficult due to differences in experimental set up, but Lee et al. (2011) managed to discriminate between most algal species with as little as two bands despite attenuation from the overlying water column. The suitable wavelengths found in their study related to variations in colour and presence of unhealthy cellular structures. They mostly fall outside the wavelength ranges found in this study, which is most likely due to the rather different vegetation types that they looked at. To discriminate between Eelgrass and associated bottom types in non-water corrected remote sensing images of much deeper marine conditions (1-30m) O'Neill et al. (2011) needed ten bands of 4 nm bandwidth. In their analysis they include spectral derivatives (R') and band ratios. Using the same data corrected for water depth they only needed 3 bands, though a classification based on these bands turned out to be less accurate. Their findings included bands covering the peak (R'566) and shoulders (500-530 & R'580) of the green reflectance maxima. This corresponds with the findings of this study, which identified significant ANOVA results in the green wavelength region and bands from this region were included in the selections with the highest J-M distance values. Their data did not include wavelengths beyond 800nm, which have proven most effective in this study.

CART analysis applied to the spectra on canvas consistently selected the 711nm band to separate between the 'green' and the 'red' (milfoil) macrophytes, followed by bands of blue light (460 - 480nm) to further separate between the two 'green' species. The latter bands fall outside the range selected as significant with the ANOVA test. CART analysis applied to the significant wavelengths of submerged species produces better J-M values than CART applied to all wavelengths. The bands selected in the latter case are also mostly from the green light region and IR wavelengths beyond 950nm. The highest J-M distance values were not achieved for band combinations selected through CART and also not always for band combinations taken from the statistically significant regions. Although distances were not calculated for all band combinations, this suggests that the combined

ANOVA and CART band selection method may not be suitable as a data dimensionality reduction method in this situation. To confirm this analysis should be repeated with other band selection methods.

OBIA species discrimination

The first part of the analysis showed how the macrophyte species Pondweed and Water Crowfoot are spectrally so similar that even without water column influences they are difficult to distinguish. These results indicate that information other than spectral reflectance needs to be incorporated in image analysis to enable accurate classification of these species. The subsequent testing of difference between species based on a number of texture and shape features confirms the potential to do so. The good performance of the 'length/width ratio of sub-objects' feature confirms that our initial visual interpretation of the image data was good and that such expert knowledge can be useful for species discrimination. The feature does however not perform very well for the images taken from the highest platform. This could indicate that the possibility to use the length/width shape feature to discriminate the species deteriorates at a less detailed scale. Sufficient resolution may be needed to produce the more elongated object shapes for Water Crowfoot during segmentation.

In general contrast features performed well, which confirmed visual interpretation of the images showing clear variation in spectral contrast amongst the two species. The spectral features perform worst with some not allowing discrimination of the species at any scale (e.g. red band). This result corresponds to some extent with the ANOVA test results which showed only narrow regions of wavelengths with sufficient difference between the macrophyte species. The best performing bands however do not seem to correspond exactly with the significant wavelength regions (e.g. blue band). The poor performance of the spectral features in general does support the original expectation that incorporation of shape and texture information is essential for successful classification of SAV. It is however unclear why there is considerable variation in separability amongst the different image scales as the spectral features are not expected to be scale dependent.

In general images produced with the Helikite were of reasonable quality, but only the images taken from the tripod and the bridge were consistently of good quality. In particular collection of NIR photos from the more elevated platforms was difficult due to limited availability of the camera autofocus in combination with the light blocking filters. The NIR(R72) band of the image taken from the pole was especially blurry, which may have affected some of the results. Texture features are likely to be more dependent on image focus than shape features like the l/w ratio, but further investigations of such effects is required. No pre-processing was applied to any of the data. Some preprocessing could have further improved data quality, as sunglint caused locally high reflectance values in most image bands. The high values will have affected contrast calculations, resulting in an overestimation of object contrast. Its quantitative effect on the presented results is currently not known.

The first attempt to use an UAS to collect remote sensing data for submerged macrophyte monitoring was not overly successful. This was to a large extent due to the type of UAS and multi-spectral sensor used. Due to a combination of camera weight, wind conditions, presence of surrounding vegetation, people and telegraph lines it was impossible to achieve elevations higher than the telescopic pole with the Helikite and therefore scale wise this platform did not contribute extra information to this study and the range of scales studied was limited. Because the exact location of the camera from this platform was most difficult to control, only a very small section of the images was ultimately suitable for analysis. It also made manual image correction rather challenging. The Helikite required restricted environmental conditions, especially when paired with a relatively heavy camera.

Similar to the spectral discrimination analysis, the object-based features may 'interact' and perform better when a number of different features are combined to discriminate between plant species. This has currently not been attempted yet. So far the difference tests are statistical exercise only. Better results are also likely with the inclusion of band ratios. To find out to what extent the features really enable accurate classification of the macrophyte species will need further testing on more extensive image data, covering larger areas and a wider range of situations.

Implications

The foregoing discussion suggests that it is not possible to accurately map submerged aquatic vegetation in the chalk streams, using spectral information only, even if water depth correction of the vegetation spectra is possible. However, despite strongly increasing K_d the NIR wavelengths still show considerable amounts of reflectance at the submergence depths observed for the chalks stream macrophyte species. The observation that wavelengths between 920 and 950nm showed potential to discriminate between at least two of the submerged species, was remarkable and use of this wavelength region should be further explored. Although spectral separability in the NIR wavelengths was not clearly confirmed by J-M distance analysis, the information in any case enhances shape and textural variation in the data, which benefits the OBIA approach. The inclusion of texture and shape features in image analysis through OBIA clearly shows promise for the mapping of SAV from image data. Further work is however also required on scale dependency, as shape and texture features did not show significant differences between the species for all scale levels.

Finally, to make the presented techniques interesting for river managers for mapping and monitoring of SAV patterns in small streams the proposed approach will need to be converted into a tool that can produce consistent results for a wide range of fluvial situations with the smallest amount of input from operators. The OBIA approach has already shown to be a useful approach in other settings, by eliminating the need for an image data sample for classification after a rule set has been created (e.g. Walker and Blaschke, 2008). Based on the results of this study it is not inconceivable that a similar tool can be developed for the benefit of shallow clear stream environments.

Acknowledgments

The fieldwork for this project was funded by the University of Worcester and the Earth and Space Foundation. The field spectroradiometer was obtained on loan from the NERC Field Spectrometry Facility (FSF) (loan ref 569.1208 and 550.1207). Furthermore we would like to thank Langford Trust Nature Reserve for access to the River Wylye field site and Justin Kirby for his help with the fieldwork.

References

Adam, E., Mutanga, O., 2009. Spectral discrimination of papyrus vegetation (Cyperus papyrus L.) in swamp wetlands using field spectrometry. ISPRS Journal of Photogrammetry and Remote Sensing. 64, 612-620.

Blaschke, T., Johansen, K., Tiede, D., 2011. Object based image analysis for Vegetation mapping and Monitoring. In: Weng, Q. (Ed.): Advances in Environmental Remote Sensing: Sensors, Algorithms, and Applications. Taylor & Francis, London, 241-271.

Breiman, L., Friedman, J.H., Olshen, R.A., Stone, C.J., 1984. Classification and Regression Trees. Chapman & Hall (Wadsworth, Inc.), New York.

Dekker, A.G., Phinn, S.R., Anstee, J., Bissett P., Brando, V.E., Casey, B., Fearns, P., Hedley, J., Klonowski, W., Lee, Z.P., Lynch, M., Lyons, M., Mobley, C., Roelfsema, C., 2011. Intercomparison of shallow water bathymetry, hydro-optics, and benthos mapping techniques in Australian and Caribbean coastal environments. Limnology and Oceanography-Methods. 9, 396-425. DOI: 10.4319/lom.2011.9.396

ENVI, 2004. ENVI User’s Guide, ENVI Version 4.1. Research Systems Inc.

Flynn, N.J., Snook, D.L., Wade, A.J,. Jarvie, H.P., 2002 Macrophyte and periphyton dynamics in a UK Cretaceous chalk stream: the River Kenneth a tributary of the Thames. The Science of the Total Environment. 282-283, 143-257.

Giardino, C., Candiani, G., Bresciani, M., Lee, Z., Gagliano, S., Pepe, M., 2012. BOMBER: A tool for estimating water quality and bottom properties from remote sensing images. Computers & Geosciences. 45, 313–318. DOI: 10.1016/j.cageo.2011.11.022

Gilvear, D., Hunter, P., Higgins, T., 2007. An experimental approach to the measurement of the effects of water depth and substrate on optical and near infra-red reflectance: a field-based assessment of the feasibility of mapping submerged instream habitat. International Journal of Remote Sensing. 28 (10), 2241-2256.

Haralick, R.M., Shanmugam, K., Dinstein, I., 1973. Textural Features for Image Classification Systems. IEEE Transactions on Man and Cybernetics. 3 (6), 610 – 621.

Hedley, J.D., Roelfsema, C.M., Phinn, S.R., Mumby, P.J., 2012. Environmental and Sensor Limitations in Optical Remote Sensing of Coral Reefs: Implications for Monitoring and Sensor Design. Remote Sensing. 4, 271-302. DOI: 10.3390/rs4010271

Hill, R.A., O'Hare, M.T., Stillman, R.A., Gozlan, R.E., 2009. Hyperspectral remote sensing of river macrophyte vegetation: towards an assessment of wildfowl and fish habitat quality. In: Proceedings of the RSPSoc Annual Conference: New Dimensions in Earth Observation, 8-11 September 2009, Leicester.

Karpouzli, E., Malthus, T.J., Place, C.J., 2004. Hyperspectral discrimination of coral reef benthic communities in the western Caribbean. Coral Reefs. 23, 141-151. DOI: 10.1007/s00338-003-0363-9

Laliberté, A.S., Rango, A., 2009. Texture and scale in object-based analysis of subdecimeter resolution UAV imagery. IEEE Transactions on Geoscience and Remote Sensing. 47(3), 761-770.

Lee, B.S., McGwire, K.C., Fritsen, C.H., 2011. Identification and quantification of aquatic vegetation with hyperspectral remote sensing in western Nevada rivers, USA. International Journal of Remote Sensing. 32, 9093-9117.

Legleiter, C.J., Roberts, D.A., 2009. A forward image model for passive optical remote sensing of river bathymetry. Remote Sensing of Environment. 113, 1025-1045. DOI: 10.1016/j.rse.2009.01.018

Marcus, W.A., Fonstad, M.A., 2008. Optical remote mapping of rivers at sub-meter resolutions and watershed extents. Earth Surface Processes and Landforms, 33. 4-24. DOI: 10.1002/esp.1637

Maritorena, S., Morel, A., Gentili, B., 1994. Diffuse-reflectance of oceanic shallow waters - influence of water depth and bottom albedo. Limnology and Oceanography. 39, 1689-1703.

O’Hare, M.T., McGahey, C., Bissett, N., Cailes, C., Henville, P., Scarlett, P., 2010. Variability in roughness measurements for vegetated rivers near base flow, in England and Scotland. Journal of Hydrology. 385, 361-370. DOI: 10.1016/j.jhydrol.2010.02.036

O'Neill, J.D., Costa, M., Sharma, T., 2011. Remote sensing of shallow coastal benthic substrates: In situ spectra and mapping of Eelgrass (*Zostera marina*) in the Gulf Islands National Park Reserve of Canada. Remote Sensing. 3, 975-1005. DOI: 10.3390/rs3050975

Phinn, S.R., Roelfsema, C.M., Mumby, P.J., 2012. Multi-scale, object-based image analysis for mapping geomorphic and ecological zones on coral reefs. International Journal of Remote Sensing. 33, 3768-3797. DOI: 10.1080/01431161.2011.633122

Trimble, 2010. eCognition® Developer 8.64.0 user guide, Trimble: Munich, Germany.

Van der Werff, H.M.A., Van der Meer, F.D., 2008, Shape-based classification of spectrally identical objects. ISPRS Journal of Photogrammetry and Remote Sensing. 63 (2), 251-258.

Urbanski, J.A., Mazur, A., Janas, U., 2009. Object-oriented classification of QuickBird data for mapping seagrass spatial structure. Oceanological and Hydrobiological Studies. 38, 27-43. DOI: 10.2478/v10009-009-0013-9

Vahtmäe, E., Kutser, T., Martin, G., Kotta, J., 2006. Feasibility of hyperspectral remote sensing for mapping benthic macroalgal cover in turbid coastal waters - a Baltic Sea case study. Remote Sensing of Environment. 101, 342-351. DOI: 10.1016/j.rse.2006.01.009

Visser, F., Hill, R.A., 2011. Application of hyperspectral image data for species detection and biomass estimation of submerged macrophytes in UK chalk streams. In: Proceedings of the EARSeL 7th SIG-Imaging Spectroscopy Workshop, Edinburgh, UK, 11-13 April 2011.

Visser, F., Wallis, C., 2010. Object-based analysis and multispectral low-altitude remote sensing for low-cost mapping of chalk steam macrophytes. The International Archives of the Photogrammetry, Remote Sensing and Spatial Information Sciences. XXXVIII-4/C7.

Walker, J. S., Blaschke, T., 2008. Object-based land-cover classification for the Phoenix metropolitan area: optimization vs. transportability. International Journal of Remote Sensing. 29 (7), 2021-2040.

Wang, C., Philpot, W.D., 2007. Using airborne bathymetric lidar to detect bottom type variation in shallow waters. Remote Sensing of Environment. 106, 123-135. DOI: 10.1016/j.rse.2006.08.003

Yang, Y., Xiao, Y., Segal, M., 2005. Identifying differentially expressed genes from microarray experiments via statistic synthesis. Bioinformatics. 21, 1084-1093. DOI: 10.1093/bioinformatics/bti108

Figure captions

Figure 1: The transmission spectra of BP1 bandpass and CC1 and R72 blocking filters based on manufacturers specifications (maxmax.com). Submerged macrophyte spectrum included with dashed line for illustration.

Figure 2: Close-up of sub-objects in ‘from tripod’ image. Left: Pondweed objects. Right: more elongated Water Crowfoot objects.

Figure 3: Attenuation of reflectance from Water Crowfoot for submergence depths between 1.5 and 40cm (example based on data collected during this study).

Figure 4: Frequency of statistically significant differences between three submerged macrophyte species with ANOVA analysis. Bars show number of significantly different combinations obtained (dark grey 99%; light grey 95%). Spectra represent min, max and average signatures for each of the species.

Figure 5: Frequency of statistically significant differences for three out-of–the-water macrophyte species with ANOVA analysis. Bars show number of significantly different combinations (dark grey 99% significant; light grey 95% significant).

Figures 6 A-D: A selection of image ‘bands’ with segmentation object outlines: A) from tripod NIR(R72) band; B) from bridge Green band; C) from pole NIR(BP1) band; D) from helikite NIR(R72) band. In all images white object outlines represent Pondweed, grey Water Crowfoot and black Unclassified.

Figure 7: Boxplots illustrating the object feature values for 8 features (A-H), comparing Pondweed and Water Crowfoot objects as derived from images taken from four different platforms.

TABLES

Table 1: Type and number of submerged vegetation spectral samples

Macrophyte species	N	Depth range (cm)
Pondweed	60	10-25
Water Crowfoot	37	2-40
Water Milfoil	66	3-50

Table 2: Results of the Jeffries-Matusita distance analysis for combinations of submerged Pondweed, Water Crowfoot and Spiked Water Milfoil. White font indicates highest achieved distance value for discriminating a pair of species; intermediate grey shade indicates highest distance value for given band combination; light grey second best.

No. Bands	Band selection method	Wavelengths (nm)	J-M distance value for species combination		
			Pondweed - Milfoil	Crowfoot - Milfoil	Pondweed - Crowfoot
2	Random from significant wavelengths	555; 935	**1.08**	**0.61**	**0.40**
	Random from all wavelengths	1054; 426	0.54	0.10	0.30
		609; 816	0.67	0.45	0.09
3	Random from significant wavelengths	935; 544; 555	1.40	0.82	**0.75**
	Random from all wavelengths	848; 539; 489	**1.45**	**1.21**	0.34
		912; 756; 884	1.08	0.61	0.48
4	CART with all wavelengths	545; 576; 966; 555	1.54	1.31	0.66
	CART with all wavelengths; No Milfoil	533; 689; 997; 550	1.61	1.18	0.85
	Random from significant wavelengths	577; 927; 919; 568	1.69	**1.37**	0.88
		553; 923; 914; 525	**1.72**	1.15	**1.14**
	Random from all wavelengths	868; 522; 892; 1011	0.97	0.58	0.42
		830; 639; 813; 773	1.08	0.96	0.28
5	CART with significant wavelengths	543; 926; 555; 537; 923	1.72	1.20	1.26
	Random from significant wavelengths	535; 925; 914; 554; 540	1.78	1.40	1.25
		562; 925; 540; 891; 573	1.72	1.49	0.87
	Random from all wavelengths	935; 559; 939; 544; 555	1.77	**1.51**	1.10
		469; 911; 562; 514; 703	**1.81**	1.33	**1.62**
6	CART with significant wavelengths; No Milfoil	533; 525; 923; 553; 913; 917	1.80	1.53	1.27
	Random from significant wavelengths	535; 919; 548; 575; 924; 561	**1.87**	1.60	**1.45**
	Random from all wavelengths	920; 566; 925; 914; 554; 540	1.84	**1.66**	1.40

Table 3: Results of the Jeffries-Matusita distance analysis for combinations of Pondweed, Water Crowfoot and Spiked Water Milfoil measured on canvas sheet. White font indicates highest achieved distance value for discriminating a pair of species; intermediate grey shade indicates highest distance value for given band combination; light grey second best.

No. Bands	Band selection method	Wavelengths (nm)	J-M distance value for species combination		
			Pondweed - Milfoil	Crowfoot - Milfoil	Pondweed - Crowfoot
3	CART with all wavelengths	711; 465; 483	1.84	1.69	0.73
	CART with all wavelengths; No Milfoil	465; 535; 483	**2.00**	1.93	0.77
4	Random from all wavelengths	545; 576; 966; 555	2.00	**1.99**	1.18
	Random from significant wavelengths	710; 752; 522; 834	2.00	1.98	1.26
5	Random from all wavelengths	543; 926; 555; 537; 923	2.00	1.98	**1.44**

Table 4. Object sample numbers N for each macrophyte and location.

	N Pond-weed	N Water Crowfoot
From tripod	12	21
From bridge	2	14
From helikite	3	8
From pole	6	9

Table 5. Results for the Mann-Whitney U non-parametric test of similarity. Shaded results are significant at 95%.

Location	Test statistic Significance	Mean R	Mean G	Mean B	Mean BP1	Mean R72	Mean R72+BP1
from tripod (1.5m)	U	108	57	68	131	113	121
	p	0.50	0.00	0.02	0.68	0.41	0.75
from bridge (3m)	U	7	7	9	6	8	5
	p	0.33	0.33	0.50	0.27	0.42	0.20
from helikite (~5m)	U	3	7	9		0	
	p	0.12	0.38	0.83		0.02	
from pole (5.4m)	U	20	16	9	15	10	16
	p	0.46	0.22	0.04	0.18	0.05	0.22

Location	Test statistic Significance	Mean Length/Width sub-objects	Mean Stdev Red Sub-objects	Stdev Red	GLCM Contrast (quick 8/11) (all dir.)	GLCM Dissimilarity (quick 8/11) (all dir.)	GLCM Homogeneity (quick 8/11) (all dir.)
from tripod (1.5m)	U	16	30	46	25	27	33
	p	0.00	0.00	0.00	0.01	0.00	0.00
from bridge (3m)	U	1	4	7	4	6	7
	p	0.03	0.15	0.33	0.15	0.27	0.33
from helikite (~5m)	U	0	2	7	2	2	2
	p	0.02	0.07	0.37	0.07	0.07	0.07
from pole (5.4m)	U	22	8	11	1	3	3
	p	0.61	0.03	0.07	0.00	0.00	0.00

Figures

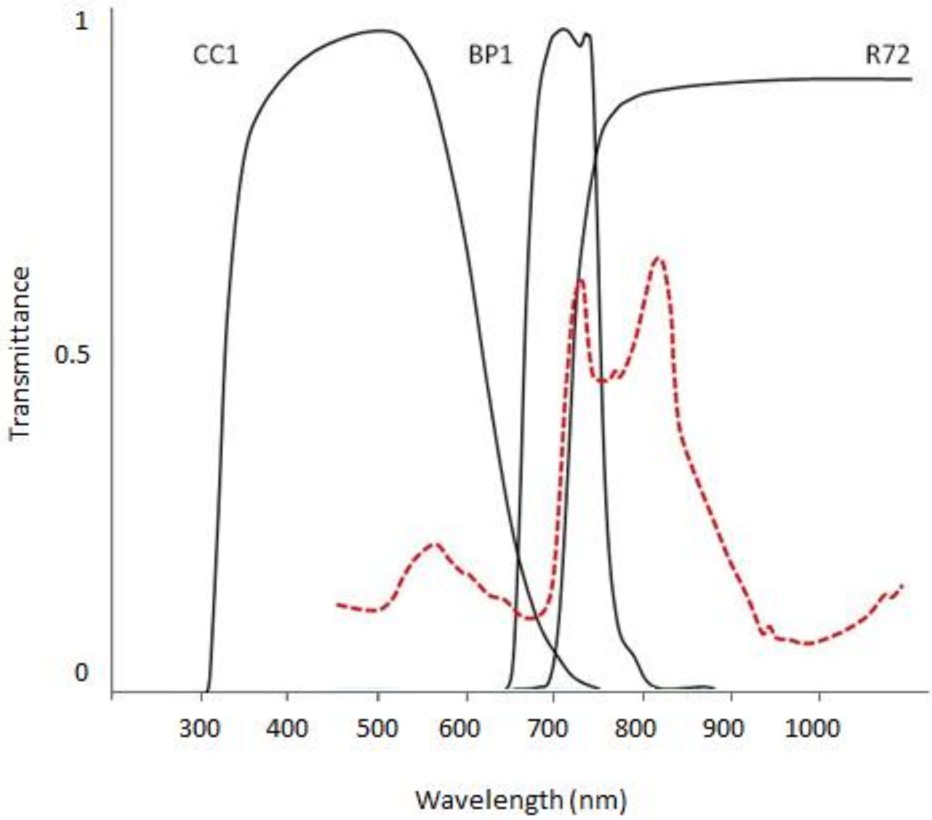

Figure 1

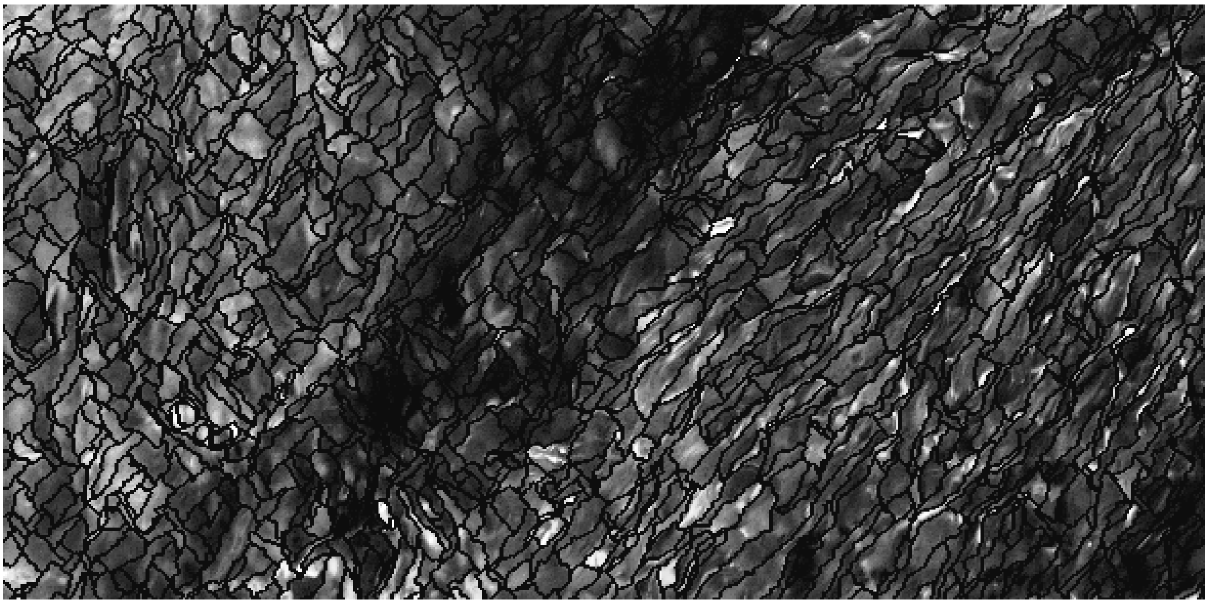

Figure 2

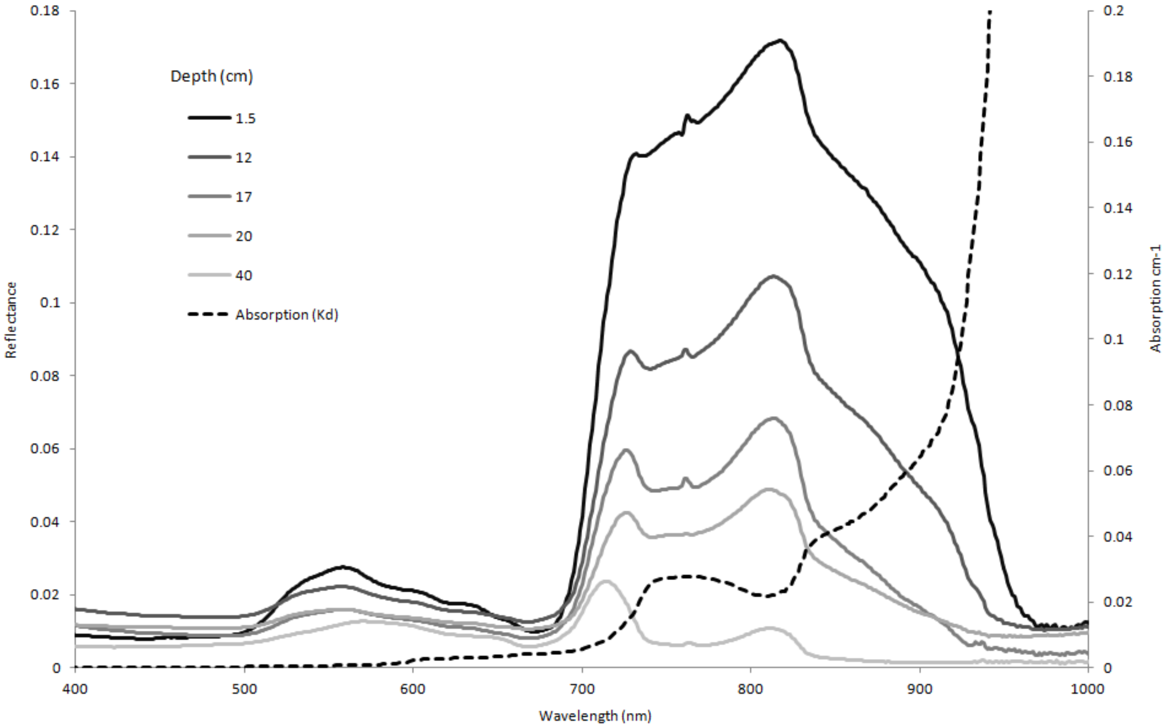
Depth (cm)
1.5
12
17
20
40
Absorption (Kd)
Reflectance
Absorption cm-1
Wavelength (nm)
0.18
0.16
0.14
0.12
0.1
0.08
0.06
0.04
0.02
0
0.2
400
500
600
700
800
900
1000

Figure 3

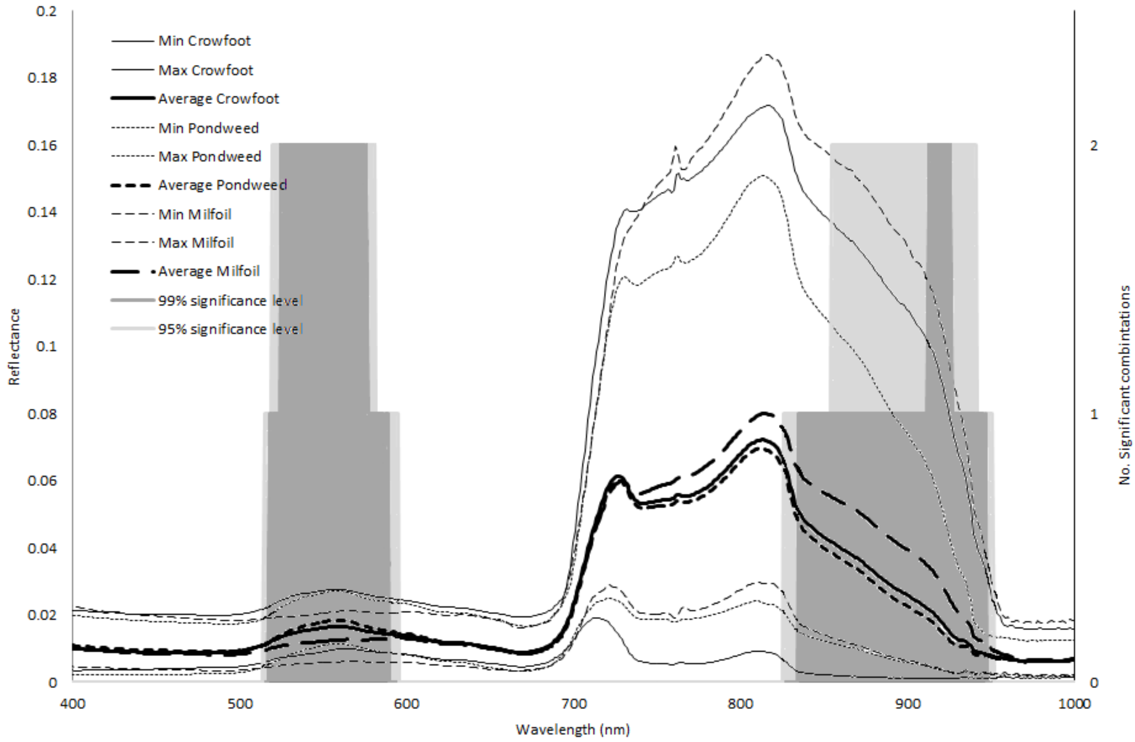
Min Crowfoot
Max Crowfoot
Average Crowfoot
Min Pondweed
Max Pondweed
Average Pondweed
Min Milfoil
Max Milfoil
Average Milfoil
99% significance level
95% significance level
Reflectance
No. Significant combintations
Wavelength (nm)
0.2
0.18
0.16
0.14
0.12
0.1
0.08
0.06
0.04
0.02
0
2
1
0
400
500
600
700
800
900
1000

Figure 4

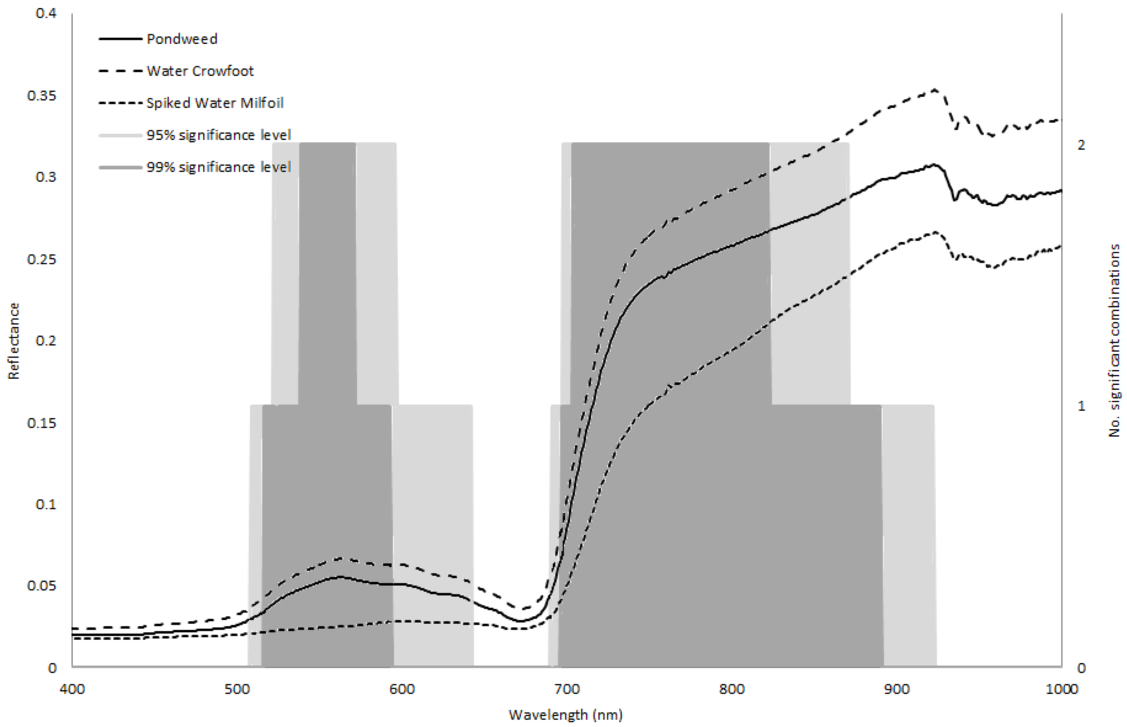
Pondweed
Water Crowfoot
Spiked Water Milfoil
95% significance level
99% significance level
Reflectance
No. significant combinations
Wavelength (nm)
0
0.05
0.1
0.15
0.2
0.25
0.3
0.35
0.4
400
500
600
700
800
900
1000
1
2

Figure 5

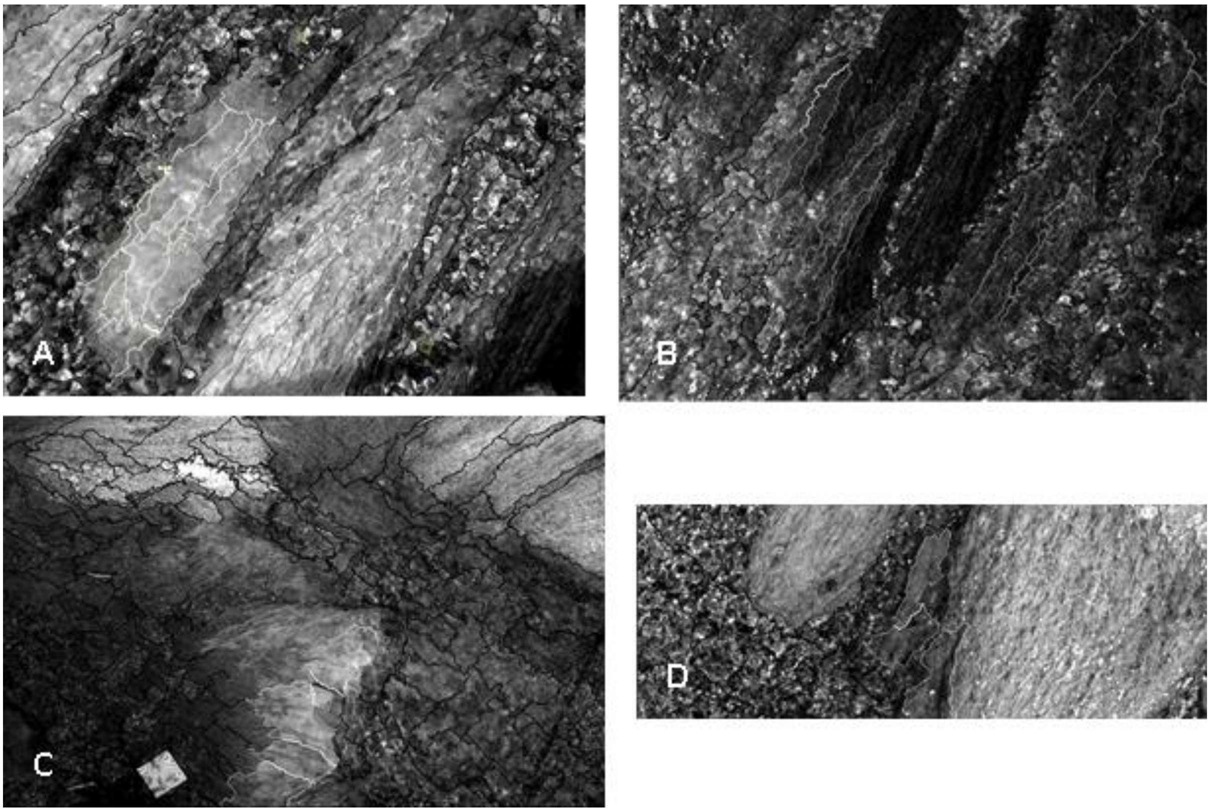

Figure 6

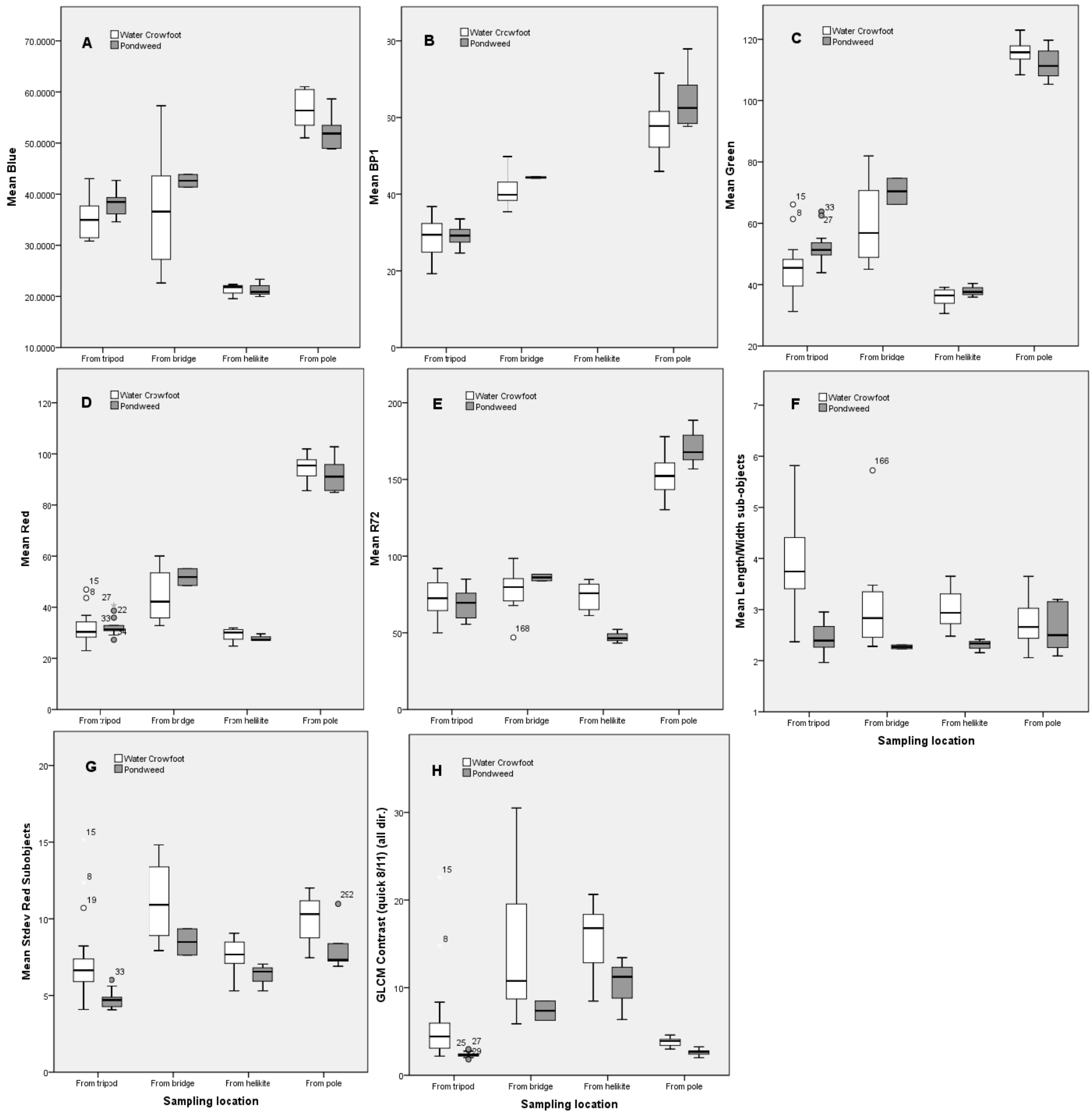
A
B
C
D
E
F
G
H
Water Crowfoot
Pondweed
Mean Blue
Mean BP1
Mean Green
Mean Red
Mean R72
Mean Length/Width sub-objects
Mean Stdev Red Subobjects
GLCM Contrast (quick 8/11) (all dir.)
From tripod
From bridge
From helikite
From pole
Sampling location

Figure 7